New Extraction of the Cosmic Birefringence from the Planck 2018 Polarization Data

Yuto Minami[*]

High Energy Accelerator Research Organization, 1-1 Oho, Tsukuba, Ibaraki 305-0801, Japan

Eiichiro Komatsu[†]

Max Planck Institute for Astrophysics, Karl-Schwarzschild-Str. 1, D-85748 Garching, Germany and
Kavli Institute for the Physics and Mathematics of the Universe (Kavli IPMU, WPI),
Todai Institutes for Advanced Study, The University of Tokyo, Kashiwa 277-8583, Japan
(Dated: November 24, 2020)

We search for evidence of parity-violating physics in the Planck 2018 polarization data, and report on a new measurement of the cosmic birefringence angle, β. The previous measurements are limited by the systematic uncertainty in the absolute polarization angles of the Planck detectors. We mitigate this systematic uncertainty completely by simultaneously determining β and the angle miscalibration using the observed cross-correlation of the E- and B-mode polarization of the cosmic microwave background and the Galactic foreground emission. We show that the systematic errors are effectively mitigated and achieve a factor-of-2 smaller uncertainty than the previous measurement, finding $\beta = 0.35 \pm 0.14$ deg (68% C.L.), which excludes $\beta = 0$ at 99.2% C.L. This corresponds to the statistical significance of 2.4σ.

INTRODUCTION

Violation of symmetry in a physical system under parity transformation is sensitive to new physics beyond the standard model (SM) of elementary particles and fields. So far, parity violation has been observed only in the weak interaction [1, 2]. In the SM of cosmology, called the Λ cold dark matter (ΛCDM) model, the energy budget of the present-day Universe is dominated by unidentified dark matter and dark energy [3]. If dark matter and energy originate from new physics beyond the SM, do either or both of them violate parity?

Polarization of the cosmic microwave background (CMB) is sensitive to parity-violating physics. Combinations of the Stokes parameters of linear polarization measured in a direction of $\hat{n}$, $Q(\hat{n}) \pm iU(\hat{n})$, transform as a spin ± 2 quantity under rotation of $\hat{n}$. We can use the spin-2 spherical harmonics to decompose these into the so-called E- and B-mode polarization as $Q(\hat{n}) \pm iU(\hat{n}) = -\sum_{\ell m}(E_{\ell m} \pm iB_{\ell m})_{\pm 2}Y_{\ell m}(\hat{n})$ [4, 5]. Under parity transformation $\hat{n} \to -\hat{n}$, the coefficients transform as $E_{\ell m} \to (-1)^{\ell}E_{\ell m}$ and $B_{\ell m} \to (-1)^{\ell+1}B_{\ell m}$. When defining angular power spectra as $C_{\ell}^{AA'} \equiv (2\ell+1)^{-1}\sum_m A_{\ell m}A'^{*}_{\ell m}$ with $A = \{E, B\}$, then C_{ℓ}^{EE} and C_{ℓ}^{BB} are invariant under parity transformation, whereas the cross-power spectrum, C_{ℓ}^{EB}, changes the sign. Therefore, nonzero values of C_{ℓ}^{EB} indicate parity violation [6].

Pseudoscalar, "axionlike" fields, ϕ, can act as dark matter, energy, or both (see [7, 8] for reviews). A Chern–Simons coupling of a time-dependent $\phi(t)$ to the electromagnetic tensor and its dual, $\frac{1}{4}g_{\phi\gamma}\phi F_{\mu\nu}\tilde{F}^{\mu\nu}$, in the Lagrangian density rotates the plane of linear polarization of photons [9–11]. This effect, called the "cosmic birefringence," rotates the CMB linear polarization by an angle $\beta = \frac{1}{2}g_{\phi\gamma}\int_{t_{\rm LSS}}^{t_0} dt\ \dot{\phi}$, and yields a nonzero observed EB spectrum as $C_{\ell}^{EB,o} = \frac{1}{2}\sin(4\beta)(C_{\ell}^{EE} - C_{\ell}^{BB})$ [6, 12–14],

where the subscript "o" denotes the observed value, the spectra on the right-hand side the intrinsic EE and BB spectra at the last scattering surface (LSS), and t_0 and $t_{\rm LSS}$ the times at present and LSS, respectively.

To determine β, we must know the polarization-sensitive directions of detectors at the focal plane with respect to the sky coordinates. This requires accurate calibration of the polarization angles. Any remaining miscalibration angle, α, leads to the same effect as isotropic β, i.e., β and α are degenerate in CMB [15–17]. Recent determinations include $\alpha + \beta = -0.36 \pm 1.24$ deg from the Wilkinson Microwave Anisotropy Probe (WMAP) [18], 0.31 ± 0.05 deg from the Planck mission [19], -0.61 ± 0.22 deg from POLARBEAR [20], 0.63 ± 0.04 deg from the South Pole Telescope (SPTpol) [21], and 0.12 ± 0.06 deg [22] and 0.09 ± 0.09 deg [23] from the Atacama Cosmology Telescope (ACT) (also see [24] for a summary of other experiments). Here the error bars show the 68% confidence levels (C.L.) for the statistical uncertainty. To isolate β, an independent estimation of α is required. For WMAP and Planck the ground calibration yields the systematic uncertainty of $\sigma_{\rm syst}(\alpha) = 1.5°$ and $0.28°$, whereas the estimates of systematic uncertainty are not yet available for POLARBEAR, SPTpol, and ACT.

There is no evidence for nonzero β so far. For the Planck measurement $\sigma_{\rm syst}(\alpha) = 0.28°$ is the dominant source of uncertainty for β. How do we make progress in distinguishing between β and α? In Refs. [25–27] we showed that we can simultaneously determine α and β if we use the CMB and Galactic foreground emission, as both are rotated by α, whereas only the CMB is rotated by β. Our method thus relies on the different frequency and multipole dependence of the CMB and foreground polarization power spectra. In this Letter, we use this new method to recalibrate the Planck high frequency instrument (HFI) detectors [28] and measure the cosmic

birefringence angle, β, with a smaller total uncertainty.

To this end, we assume that there was no intrinsic EB correlation of CMB at the LSS. However, the intrinsic CMB EB can be accounted for if necessary; as such, intrinsic C_ℓ^{EB} usually has very different ℓ dependence (e.g., [29]). For the baseline result we also assume that there is no intrinsic EB correlation of the foreground, but we relax this assumption towards the end of the Letter.

MAPS TO CROSS POWER SPECTRA

We use Planck maps from the third public release, referred to as "PR3". We analyze the polarization maps in four polarized Planck HFI channels: $\nu \in \{100, 143, 217, 353\}\,$GHz. We also use the temperature maps when we correct the temperature-to-polarization $(I \to P)$ leakage effect due to beams. We cross-correlate four frequency maps from different half-mission (HM) maps, HM1 and HM2, to reduce the correlated systematics and bias from the auto correlation noise.

To reject spurious signals, we apply three types of masks. (1) Bad pixels: we remove the pixels that were not observed by any detectors. (2) Bright CO emission: the Planck team used the bandpass templates to correct for CO emission, which were generated at $N_{\rm side} = 128$ in the HEALPix format [30]. The difference between this and the native resolution of the HM maps ($N_{\rm side} = 2048$) causes a bias, which is significant in bright CO emission regions. To reduce the bias, we follow Planck team's suggestion and mask the bright CO regions where the bias level is larger than 1% of the noise level [28]. We have applied this mask to all channels except for $143\,$GHz channel, to which no CO bandpass template was applied. (3) Bright point sources: we use the point-source mask provided by the Planck team, which removes sources with polarization detection significance levels of $\geq 99.97\%$.

We apply the combined masks to the HM maps. We then estimate observed power spectra, $C_\ell^{XY,\rm o}$, with $XY \in \{TT, EE, BB, TE, ET, EB, BE\}$ from 16 combinations of the masked HM maps using the NaMaster package [31]. When estimating $C_\ell^{XY,o}$ we apodize the combined masks with $0.5\,$deg using the "Smooth" method of NaMaster. The fractions of sky used for the analysis are calculated as $f_{\rm sky} = \sum_{i=1}^{N_{\rm pix}} w_i^2/N_{\rm pix}$, where w_i is the value of (non-integer) smoothed mask and $N_{\rm pix} = 12N_{\rm side}^2$ is the number of pixels of the HM maps. We find $(f_{\rm sky}^{\nu,\rm HM1}, f_{\rm sky}^{\nu,\rm HM2}) = \{(0.97, 0.95), (0.94, 0.90), (0.82, 0.77), (0.92, 0.89)\}$ for $\nu \in \{100, 143, 217, 353\}\,$GHz, respectively.

To remove the $I \to P$ leakage, we use the beam window matrix, $W_\ell^{XY,X'Y'}$, produced by the "QuickPol" method [32]. The matrix describes how the observed XY power spectra are related to the input ones with $X'Y' \in \{TT, EE, BB, TE\}$. Since our power spectra in-

clude both the CMB and foregrounds, we do not have a prior knowledge of the input power spectra. Therefore, we approximately use the *observed* power spectra divided by the diagonal elements of the beam window matrix as the input. In summary, the observed power spectra after the leakage subtraction are given by

$$C_\ell^{XY,\rm o} = \hspace{4cm} (1)$$

$$\hat{C}_\ell^{XY,\rm o} - W_\ell^{\rm pix,XY} \sum_{X'Y' \neq XY} \frac{W_\ell^{XY,X'Y'} \hat{C}_\ell^{X'Y',\rm o}}{W_\ell^{\rm pix,X'Y'} W_\ell^{X'Y',X'Y'}},$$

where $\hat{C}_\ell^{XY}$ is a power spectrum before the leakage subtraction, and $W_\ell^{\rm pix,XY}$ is a pixel window function for the XY power spectrum. Because QuickPol assumes that the signal is statistically isotropic on the sky, the leakage from ET is equal to that from TE; thus, we use the mean of TE and ET as an input for $X'Y' = TE$.

ESTIMATION OF α AND β

We estimate one global cosmic birefringence angle, β, and independent miscalibration angles, α_ν, at four frequencies. When the intrinsic EB power spectra of the CMB at LSS and the Galactic foregrounds vanish, we can relate the observed power spectra and the best-fitting ΛCDM CMB power spectra [33] at each ℓ as [27]

$$\mathbf{A}\vec{C}_\ell^{\rm o} - \mathbf{B}\vec{C}_\ell^{\rm CMB,th} = \mathbf{0}, \hspace{2cm} (2)$$

where $\vec{C}_\ell^{\rm o}$ is an array of the observed power spectra, $\left(C_\ell^{E_i E_j,\rm o} \;\; C_\ell^{B_i B_j,\rm o} \;\; C_\ell^{E_i B_j,\rm o}\right)^T$, with i,j in 32 combinations, $\vec{C}_\ell^{\rm CMB,th}$ is an array of the best-fitting ΛCDM CMB power spectra, $\left(C_\ell^{E_i E_j,\rm CMB,th} W_\ell^{E_i E_j, E_i E_j} W_\ell^{\rm pix,E_i E_j}\right.$ $\left. C_\ell^{B_i B_j,\rm CMB,th} W_\ell^{B_i B_j, B_i B_j} W_\ell^{\rm pix,B_i B_j}\right)^T$, with the corresponding beam window matrix, $\mathbf{A}$ is a block diagonal matrix of $\left(-\vec{R}^T(\alpha_i, \alpha_j)\mathbf{R}^{-1}(\alpha_i, \alpha_j) \;\; 1\right)$, and $\mathbf{B}$ is a block diagonal matrix of $\left(\vec{R}^T(\alpha_i + \beta, \alpha_j + \beta)\right.$ $\left. -\vec{R}^T(\alpha_i, \alpha_j)\mathbf{R}^{-1}(\alpha_i, \alpha_j)\mathbf{R}(\alpha_i + \beta, \alpha_j + \beta)\right)$. Here, $\mathbf{R}$ and $\vec{R}$ are the rotation matrix and vector defined in Eq. (8) and (9) of Ref. [27], respectively. We have 32 independent equations from 16 combinations of maps, as we have two different equations for $C_\ell^{E_i B_j,\rm o}$ and $C_\ell^{E_j B_i,\rm o}$.

In practice, we estimate α_ν and β by maximizing the log-likelihood function [27]:

$$\ln \mathcal{L} = -\frac{1}{2} \sum_{\ell=\ell_{\rm min}}^{\ell_{\rm max}} \vec{v}_\ell^T \mathbf{C}_\ell^{-1} \vec{v}_\ell, \hspace{1.5cm} (3)$$

where $\vec{v}_\ell \equiv \mathbf{A}\vec{C}_\ell^{\rm o} - \mathbf{B}\vec{C}_\ell^{\rm CMB,th}$ and $\mathbf{C}_\ell \equiv \mathbf{A}\,{\rm Cov}(\vec{C}_\ell^{\rm o}, \vec{C}_\ell^{\rm oT})\mathbf{A}^T$. We use a publicly available

Markov chain Monte Carlo sampler EMCEE [34] to obtain posterior distributions of α_ν and β with this likelihood and flat priors on α_ν and β. As we estimate the covariance matrix from the observed power spectra, we use binned power spectra with $\Delta\ell = 20$ to reduce the statistical fluctuation in the covariance matrix. We follow the definition of $\mathrm{Cov}(\vec{C}_\ell^{\mathrm{o}}, \vec{C}_\ell^{\mathrm{o}T})$ given in Eqs. (12)-(15) of Ref. [27], but with a slight modification to account for the effect of mask. Specifically, we divide the covariance matrix by $f_{\mathrm{sky}}^{\mathrm{eff}} = \sqrt[4]{f_{\mathrm{sky}}^i f_{\mathrm{sky}}^j f_{\mathrm{sky}}^p f_{\mathrm{sky}}^q}$ with f_{sky}^i being f_{sky} for the ith map.

Our covariance matrix formula is valid for approximately Gaussian random fields; however, non-Gaussian effects from, e.g., the foreground, may become non-negligible at low multipoles. To find a suitable minimum multipole, ℓ_{min}, we vary ℓ_{min} from 2 to 200 and estimate α_ν and β. We obtain stable results for $\ell_{\mathrm{min}} \approx 50$. Specifically, we find $\beta = 0.71 \pm 0.14$ and 0.48 ± 0.14 deg for $\ell_{\mathrm{min}} = 25$ and 41, respectively, but then find a stable value of $\beta = 0.35$ deg to within the uncertainty for $\ell_{\mathrm{min}} \gtrsim 50$; thus, we use $\ell_{\mathrm{min}} = 51$, which coincides with the value adopted by the Planck team [19].

As for the maximum multipole, ℓ_{max}, we use the same $\ell_{\mathrm{max}} = 1500$ as in the Planck analysis [19].

VALIDATION WITH THE FULL FOCAL PLANE SIMULATION

To validate our pipeline, we first use the maps from Planck's end-to-end full focal plane 10 (FFP10) simulation [28]. Since the FFP10 simulation does not have foreground maps convolved with realistic beam effects such as the $I \rightarrow P$ leakage, we only consider CMB and noise realizations of the HM maps.

As the maps do not include the foreground, we can only estimate the combination $\alpha_\nu + \beta$. Thus, we estimate (i) α_ν by setting $\beta = 0$ deg and (ii) β by setting $\alpha_\nu = 0$ deg for 10 realizations. We expect to recover (i) $\alpha_\nu = 0$ and (ii) $\beta = 0$, as the FFP10 simulation does not include angle miscalibration or the cosmic birefringence. The means and standard deviations of the recovered angles are (i) $\alpha_\nu = \{-0.008 \pm 0.047, 0.013 \pm 0.033, 0.017 \pm 0.065, 0.14 \pm 0.41\}$ deg for $\nu \in \{100, 143, 217, 353\}$ GHz and (ii) $\beta = 0.010 \pm 0.030$ deg. We thus find no evidence for a spurious α_ν or β from the instrumental effects, to the extent that is implemented in the FFP10 simulation.

RESULTS

First, we assume that the polarization directions of the Planck detectors are perfectly calibrated, i.e., $\alpha_\nu = 0$, and estimate β. This case is similar to the Planck analysis [19], except that they measured β from foreground-

TABLE I. Cosmic birefringence and miscalibration angles from the Planck 2018 polarization data with 1σ (68%) uncertainties

Angles	Results (deg)
β	0.35 ± 0.14
α_{100}	-0.28 ± 0.13
α_{143}	0.07 ± 0.12
α_{217}	-0.07 ± 0.11
α_{353}	-0.09 ± 0.11

cleaned maps. We find $\beta(\alpha_\nu = 0) = 0.289 \pm 0.048$ deg, which is consistent with the Planck team's result, $0.29 \pm 0.05\,(\mathrm{stat.}) \pm 0.28\,(\mathrm{syst.})$ from C_ℓ^{EB}, within the statistical uncertainty. When C_ℓ^{TB} is added they find 0.31 deg. The second error bar of the Planck measurement is the systematic uncertainty in α from the ground calibration. Our goal is to estimate α_ν simultaneously to eliminate this uncertainty. Nevertheless, it is reassuring that we obtain consistent results under a similar setup.

Next, we estimate β and α_ν simultaneously. We report our baseline results in Table I, and the posterior distributions of the angles in Fig. 1. It shows that α_ν and β are anticorrelated, since the CMB determines $\alpha_\nu + \beta$ and the degeneracy is broken by the foregrounds [25]. We find that the miscalibration angles are consistent with zero to within 1σ at 143, 217, and 353 GHz, and is a 2σ level at 100 GHz. All the values are within the systematic uncertainty of the ground calibration, $\sigma_{\mathrm{syst}}(\alpha) = 0.28$ deg. Our baseline result is $\beta = 0.35 \pm 0.14$ deg, which excludes the null hypothesis by 99.2% C.L. The uncertainty no longer contains the ground calibration uncertainty, as we simultaneously determine α_ν and β. Our measurement is consistent with the Planck team's result quoted above, with a factor-of-2 smaller total uncertainty.

We show the fitted EB power spectra of 143 and 217 GHz, which have the smallest error bars, in Fig. 2. The measured data points with error bars should be compared with the sum of $C_\ell^{EE} - C_\ell^{BB}$ terms of $-\mathbf{A}\vec{C}_\ell^{\mathrm{o}}$ (red) and $\mathbf{B}\vec{C}_\ell^{\mathrm{CMB,th}}$ (blue). To guide eyes, we note that the 217 GHz-HM1×143 GHz-HM2 panel shows the EB power spectrum with a hint of the acoustic oscillation matched by the CMB E-mode power spectrum. Similar trends are seen in some of the other panels, explaining a 2.4σ hint for a nonzero value of β.

While it is perfectly consistent with the quoted systematic uncertainty of the ground calibration, one may wonder if $\alpha_{100} = -0.28 \pm 0.13$ deg is the cause for a nonzero value of β. One potential source of worry is the EB correlation of synchrotron radiation which may become important at lower ν. The intrinsic EB correlation of synchrotron, if any, may create the bias. To test this, we exclude the 100 GHz channel and repeat the analysis. We find $\beta = 0.40 \pm 0.15$ deg and $\alpha_\nu = \{0.05 \pm 0.12, -0.13 \pm 0.12, -0.10 \pm 0.11\}$ deg for
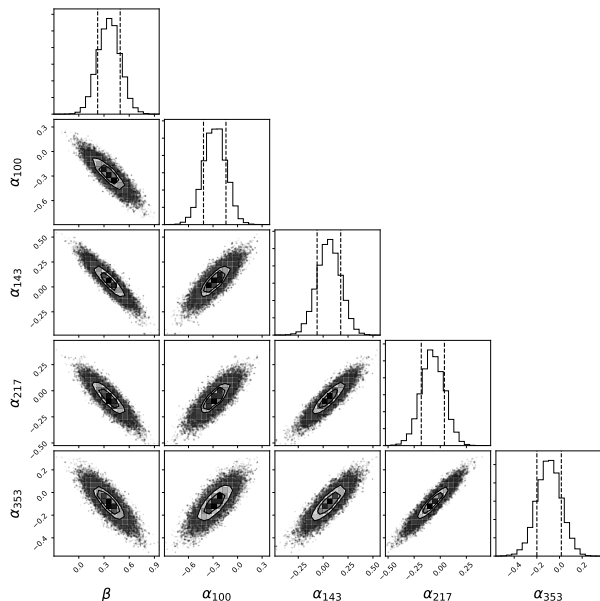
FIG. 1. Posterior distributions of β (the first column) against the miscalibration angles α_ν. The solid contour lines in the 2D histograms show 1σ (39.3%) and 2σ (86.5%) of each area. The dashed lines in the 1D histograms show 1σ (from 16% to 84%) quantiles of each area.

$\nu \in \{143, 217, 353\}$ GHz, which agree with the baseline.

We test the effect of the $I \to P$ leakage by estimating α_ν and β without the leakage subtraction. We find $\beta = 0.35 \pm 0.14$ deg and $\alpha_\nu = \{-0.25 \pm 0.14, 0.07 \pm 0.12, -0.05 \pm 0.11, -0.07 \pm 0.11\}$ deg for $\nu \in \{100, 143, 217, 353\}$ GHz, which agree with the baseline; thus, the results are robust against the leakage.

EB CORRELATION FROM THE GALACTIC FOREGROUND

So far, we have assumed that the intrinsic EB power spectrum of the foreground emission vanishes. In this section we relax this assumption. In the previous section we have shown that dropping the 100 GHz channel does not affect the result for β [35]. Therefore, we focus on the dust emission, which is the dominant foreground in the Planck HFI channels.

As discussed in Refs. [25, 26], we can parameterize the dust EB power spectrum by a frequency-dependent rotation angle, $\gamma(\nu)$, as $C_\ell^{EB,\mathrm{dust}} = \frac{\sin[4\gamma(\nu)]}{2}\left(C_\ell^{EE,\mathrm{dust}} - C_\ell^{BB,\mathrm{dust}}\right)$. The sign of the EB correlation is the same as γ because $C_\ell^{EE,\mathrm{dust}} > C_\ell^{BB,\mathrm{dust}}$ [36]. In the worst case scenario γ is independent of frequency, which would make it indistinguishable from β. Then, our result can be reinterpreted as the combination of angles $\beta - \gamma = 0.35 \pm 0.14$ deg. Because

both the TE and TB cross power spectra of thermal dust emission are positive [36], a positive EB, hence $\gamma > 0$, is expected; thus, our baseline result assuming $\gamma = 0$ gives a lower bound for β.

What if $\gamma < 0$? If all of the signal we see in β is due to the dust emission, it implies $\gamma = -0.35 \pm 0.14$ deg. In this case, assuming $\xi = C_\ell^{BB,\mathrm{dust}}/C_\ell^{EE,\mathrm{dust}} \simeq 0.5$ [36, 37], we find a correlation coefficient of $f_c = C_\ell^{EB,\mathrm{dust}}/\sqrt{C_\ell^{EE,\mathrm{dust}}C_\ell^{BB,\mathrm{dust}}} \simeq (-8.6 \pm 3.5) \times 10^{-3}$, whose absolute value corresponds to the lowest value of f_c discussed in Ref. [37].

SUMMARY AND DISCUSSION

In this Letter, we have applied the new method of simultaneously determining the cosmic birefringence angle β and miscalibration angles of detectors α_ν to the Planck 2018 data. The method was developed originally in Ref. [25] for autofrequency power spectra measured over the full sky, and has been extended to include a partial sky coverage [26] and cross-frequency spectra [27]. The idea is simple: while α_ν rotates linear polarization of both the CMB and Galactic foreground emission, β rotates only the CMB. We find that all of α_ν in the polarized Planck HFI channels are consistent with zero to within the quoted systematic uncertainty of the ground calibration of the Planck bolometers [19].

We measure $\beta = 0.35 \pm 0.14$ deg (68% C.L.), which excludes zero by 99.2% C.L. This corresponds to the statistical significance of 2.4σ. This value is consistent with the Planck team's result assuming $\alpha_\nu = 0$, but with a factor-of-2 smaller total uncertainty because our result is no longer subject to the ground calibration uncertainty.

We can constrain various models of new physics which produce a spatially uniform β. Let us consider a Lagrangian density including a Chern–Simons coupling between axionlike particles and photons (see, e.g., [38]):

$$\mathcal{L} \supset \frac{1}{4}g_{\phi\gamma}\phi F_{\mu\nu}\tilde{F}^{\mu\nu}, \tag{4}$$

where $g_{\phi\gamma}$ is a coupling constant, ϕ is an axionlike pseudoscalar field, and $F_{\mu\nu}$ and $\tilde{F}_{\mu\nu}$ are the electromagnetic tensor and its dual. The difference of the value of ϕ between the LSS and the location of the observer ("obs") rotates the plane of linear polarization of CMB photons by $\beta = \frac{1}{2}g_{\phi\gamma}(\bar{\phi}_{\mathrm{obs}} - \bar{\phi}_{\mathrm{LSS}} + \delta\phi_{\mathrm{obs}})$ [6, 9–14, 39], where $\bar{\phi}$ and $\delta\phi$ denote the mean and fluctuation of the field value, respectively. Then our measurement gives

$$g_{\phi\gamma}(\bar{\phi}_{\mathrm{obs}} - \bar{\phi}_{\mathrm{LSS}} + \delta\phi_{\mathrm{obs}}) = (1.2 \pm 0.5) \times 10^{-2}\,\mathrm{rad}. \tag{5}$$

We can use this to constrain models (see, e.g., [39]).

If our measurement of β is confirmed with higher statistical significance in future, it would have a profound implication for fundamental physics. To further test and
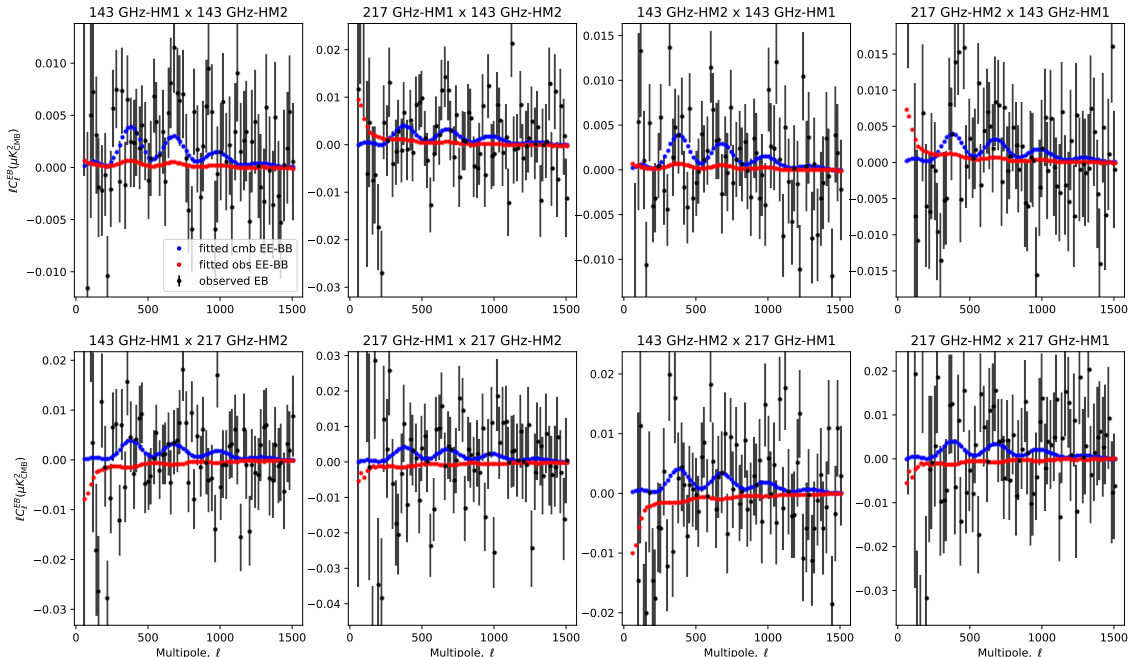
FIG. 2. Fitted EB cross spectra from 143 and 217 GHz maps. We show the measured EB data with error bars (black), $C_\ell^{EE} - C_\ell^{BB}$ terms of observed $-\mathbf{A}\vec{C}_\ell^{\text{o}}$ (red), and the CMB $\mathbf{B}\vec{C}_\ell^{\text{CMB,th}}$ (blue). The data points should be compared with the sum of $C_\ell^{EE} - C_\ell^{BB}$ terms.

improve our measurement, one can apply our method to both the ongoing [23, 40–43] and future [44–48] CMB polarization experiments.

* yminami@post.kek.jp
† komatsu@mpa-garching.mpg.de

[1] T. Lee and C.-N. Yang, Phys. Rev. **104**, 254 (1956).
[2] C. S. Wu, E. Ambler, R. W. Hayward, D. D. Hoppes, and R. P. Hudson, Phys. Rev. **105**, 1413 (1957).
[3] S. Weinberg, *Cosmology* (Oxford University Press, 2008).
[4] U. Seljak and M. Zaldarriaga, Phys. Rev. Lett. **78**, 2054 (1997), arXiv:astro-ph/9609169 [astro-ph].
[5] M. Kamionkowski, A. Kosowsky, and A. Stebbins, Phys. Rev. Lett. **78**, 2058 (1997), arXiv:astro-ph/9609132.
[6] A. Lue, L.-M. Wang, and M. Kamionkowski, Phys. Rev. Lett. **83**, 1506 (1999), arXiv:astro-ph/9812088 [astro-ph].
[7] D. J. E. Marsh, Phys. Rept. **643**, 1 (2016), arXiv:1510.07633 [astro-ph.CO].
[8] E. G. Ferreira, To appear in Astron. Astrophys. Rev. (2020), arXiv:2005.03254 [astro-ph.CO].
[9] S. M. Carroll, G. B. Field, and R. Jackiw, Phys. Rev. D **41**, 1231 (1990).
[10] D. Harari and P. Sikivie, Phys. Lett. B **289**, 67 (1992).
[11] S. M. Carroll, Phys. Rev. Lett. **81**, 3067 (1998), arXiv:astro-ph/9806099 [astro-ph].
[12] B. Feng, H. Li, M. Li, and X. Zhang, Phys. Lett. **B620**, 27 (2005), arXiv:hep-ph/0406269 [hep-ph].
[13] B. Feng, M. Li, J.-Q. Xia, X. Chen, and X. Zhang, Phys. Rev. Lett. **96**, 221302 (2006), arXiv:astro-ph/0601095 [astro-ph].

[14] G.-C. Liu, S. Lee, and K.-W. Ng, Phys. Rev. Lett. **97**, 161303 (2006), arXiv:astro-ph/0606248 [astro-ph].

[15] E. Y. S. Wu *et al.* (QUaD), Phys. Rev. Lett. **102**, 161302 (2009), arXiv:0811.0618 [astro-ph].

[16] E. Komatsu *et al.* (WMAP), Astrophys. J. Suppl. **192**, 18 (2011), arXiv:1001.4538 [astro-ph.CO].

[17] B. Keating, M. Shimon, and A. Yadav, Astrophys. J. **762**, L23 (2012), arXiv:1211.5734 [astro-ph.CO].

[18] G. Hinshaw *et al.* (WMAP), Astrophys. J. Suppl. **208**, 19 (2013), arXiv:1212.5226 [astro-ph.CO].

[19] P. C. I. XLIX (Planck), Astron. Astrophys. **596**, A110 (2016), arXiv:1605.08633 [astro-ph.CO].

[20] S. Adachi *et al.* (POLARBEAR), Astrophys. J. **897**, 55 (2020), arXiv:1910.02608 [astro-ph.CO].

[21] F. Bianchini *et al.* (SPT), Phys. Rev. D **102**, 083504 (2020), arXiv:2006.08061 [astro-ph.CO].

[22] T. Namikawa *et al.* (ACT), Phys. Rev. D **101**, 083527 (2020), arXiv:2001.10465 [astro-ph.CO].

[23] S. K. Choi *et al.* (ACT), arXiv e-prints (2020), arXiv:2007.07289 [astro-ph.CO].

[24] J. P. Kaufman, B. G. Keating, and B. R. Johnson, Mon. Not. Roy. Astron. Soc. **455**, 1981 (2016), arXiv:1409.8242 [astro-ph.CO].

[25] Y. Minami, H. Ochi, K. Ichiki, N. Katayama, E. Komatsu, and T. Matsumura, PTEP **2019**, 083E02 (2019), arXiv:1904.12440 [astro-ph.CO].

[26] Y. Minami, PTEP **2020**, 063E01 (2020), arXiv:2002.03572 [astro-ph.CO].

[27] Y. Minami and E. Komatsu, Progress of Theoretical and Experimental Physics **2020** (2020), 10.1093/ptep/ptaa130, 103E02, https://academic.oup.com/ptep/article-pdf/2020/10/103E02/34002973/ptaa130.pdf.

[28] N. Aghanim *et al.* (Planck), Astron. Astrophys. **641**, A3 (2020), arXiv:1807.06207 [astro-ph.CO].

[29] B. Thorne, T. Fujita, M. Hazumi, N. Katayama, E. Komatsu, and M. Shiraishi, Phys. Rev. **D97**, 043506 (2018), arXiv:1707.03240 [astro-ph.CO].

[30] K. M. Gorski, E. Hivon, A. J. Banday, B. D. Wandelt, F. K. Hansen, M. Reinecke, and M. Bartelman, Astrophys. J. **622**, 759 (2005), arXiv:astro-ph/0409513 [astro-ph].

[31] D. Alonso, J. Sanchez, and A. Slosar (LSST Dark Energy Science), Mon. Not. Roy. Astron. Soc. **484**, 4127 (2019), arXiv:1809.09603 [astro-ph.CO].

[32] E. Hivon, S. Mottet, and N. Ponthieu, Astron. Astrophys. **598**, A25 (2017), arXiv:1608.08833 [astro-ph.CO].

[33] We use the CMB power spectra calculated by CAMB [49] using the Planck 2018 cosmological parameters for "TT,TE,EE+lowE+lensing" [50]: $\Omega_b h^2 = 0.022\,37$, $\Omega_c h^2 = 0.1200$, $h = 0.6736$, $\tau = 0.0544$, $A_s = 2.100 \times 10^{-9}$, and $n_s = 0.9649$.

[34] D. Foreman-Mackey, D. W. Hogg, D. Lang, and J. Goodman, Publ. Astron. Soc. Pac. **125**, 306 (2013), arXiv:1202.3665 [astro-ph.IM].

[35] We further check the non-importance of the synchrotron foreground by computing EB due to synchrotron for 143 GHz-HM1$\times$217 GHz-HM2, where variance of the observed EB is small. We estimate a Gaussian variance of synchrotron EB using a synchrotron model implemented in the public code "PySM" [51]. The ratio of the synchrotron variance to the observed variance is $O(10^{-9})$. Thus, even if synchrotron has a significant EB correlation at the level of 5σ, the effect is negligible.

[36] Y. Akrami *et al.* (Planck), Astron. Astrophys. **641**, A11 (2020), arXiv:1801.04945 [astro-ph.GA].

[37] M. H. Abitbol, J. C. Hill, and B. R. Johnson, Mon. Not. Roy. Astron. Soc. **457**, 1796 (2016), arXiv:1512.06834 [astro-ph.CO].

[38] M. S. Turner and L. M. Widrow, Phys. Rev. D **37**, 2743 (1988).

[39] T. Fujita, Y. Minami, K. Murai, and H. Nakatsuka, arXiv e-prints (2020), arXiv:2008.02473 [astro-ph.CO].

[40] P. A. R. Ade *et al.* (POLARBEAR), Astrophys. J. **794**, 171 (2014), arXiv:1403.2369 [astro-ph.CO].

[41] P. Ade *et al.* (BICEP2), Astrophys. J. **792**, 62 (2014), arXiv:1403.4302 [astro-ph.CO].

[42] B. Benson *et al.* (SPT-3G), Proc. SPIE Int. Soc. Opt. Eng. **9153**, 91531P (2014), arXiv:1407.2973 [astro-ph.IM].

[43] Z. Xu *et al.*, Astrophys. J. **891**, 134 (2019), arXiv:1911.04499 [astro-ph.IM].

[44] B. Westbrook *et al.*, Journal of Low Temperature Physics **193** (2018), 10.1007/s10909-018-2059-0.

[45] H. Hui *et al.*, Proc. SPIE Int. Soc. Opt. Eng. **10708**, 1070807 (2018), arXiv:1808.00568 [astro-ph.IM].

[46] P. Ade *et al.* (Simons Observatory), JCAP **1902**, 056 (2019), arXiv:1808.07445 [astro-ph.CO].

[47] J. Carlstrom *et al.*, Bulletin of the AAS **51** (2019), https://baas.aas.org/pub/2020n7i209.

[48] M. Hazumi *et al.* (LiteBIRD), J. Low Temp. Phys. **194**, 443 (2019).

[49] A. Lewis, A. Challinor, and A. Lasenby, Astrophys. J. **538**, 473 (2000), astro-ph/9911177.

[50] N. Aghanim *et al.* (Planck), Astron. Astrophys. **641**, A6 (2020), arXiv:1807.06209 [astro-ph.CO].

[51] B. Thorne, J. Dunkley, D. Alonso, and S. Naess, Mon. Not. Roy. Astron. Soc. **469**, 2821 (2017), arXiv:1608.02841 [astro-ph.CO].